Electronic Supplementary Material (ESI) for Physical Chemistry Chemical Physics

NMR parameters in alkali, alkaline earth and rare earth fluorides from first principle calculations

Aymeric Sadoc, Monique Body, Christophe Legein, Mamata Biswal, Franck Fayon, Xavier Rocquefelte and Florent Boucher

Electronic Supplementary Information
Table of content

Experimental conditions used for ^{19}F solid state NMR spectroscopy

The ^{19}F solid-state MAS NMR experiments were conducted on Avance 300 (magnetic field of 7.0 T) and Avance 750 (magnetic field of 17.6 T) Bruker spectrometers operating at Larmor frequencies of 282.2 and 705.85 MHz, respectively, using 2.5 mm and 1.3 mm CPMAS probehead. All spectra were acquired using a Hahn echo sequence with an inter-pulse delay equal to one rotor period, except CaF_2 and LaF_3 for which a single pulse sequence was used. The recycle delays were set to 10 s for LiF, NaF, KF, RbF, CsF, MgF_2, CaF_2, SrF_2, BaF_2 and ScF_3 and 30 s for YF_3 and LaF_3. ^{19}F nutation frequencies ranging between 93 (2.5 mm prohead) and 195 kHz (1.3 mm probehead) were used. The ^{19}F chemical shifts were referenced to $CFCl_3$ at 0 ppm.

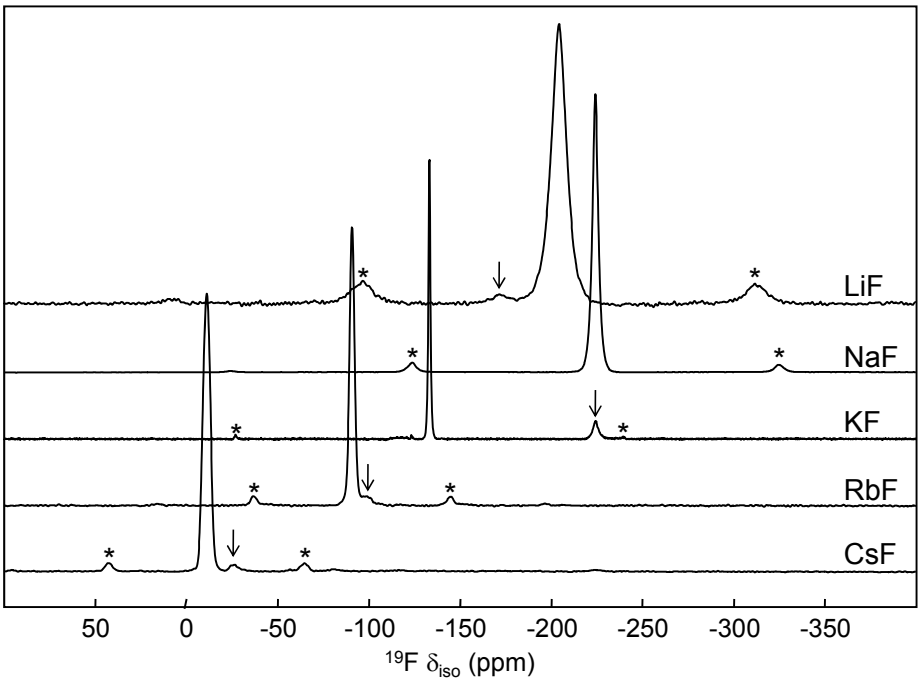

Figure S1. ^{19}F MAS NMR spectra of alkaline fluorides obtained at a magnetic field of 7.0 T using spinning frequencies of 30 kHz for LiF, 25 kHz for NaF and KF and 15 kHz for RbF and CsF. The arrows on the NMR spectra of LiF, RbF and CsF indicate unidentified impurities. The arrow on the spectrum of KF indicates an impurity identified as NaF. The asterisks indicate spinning sidebands.

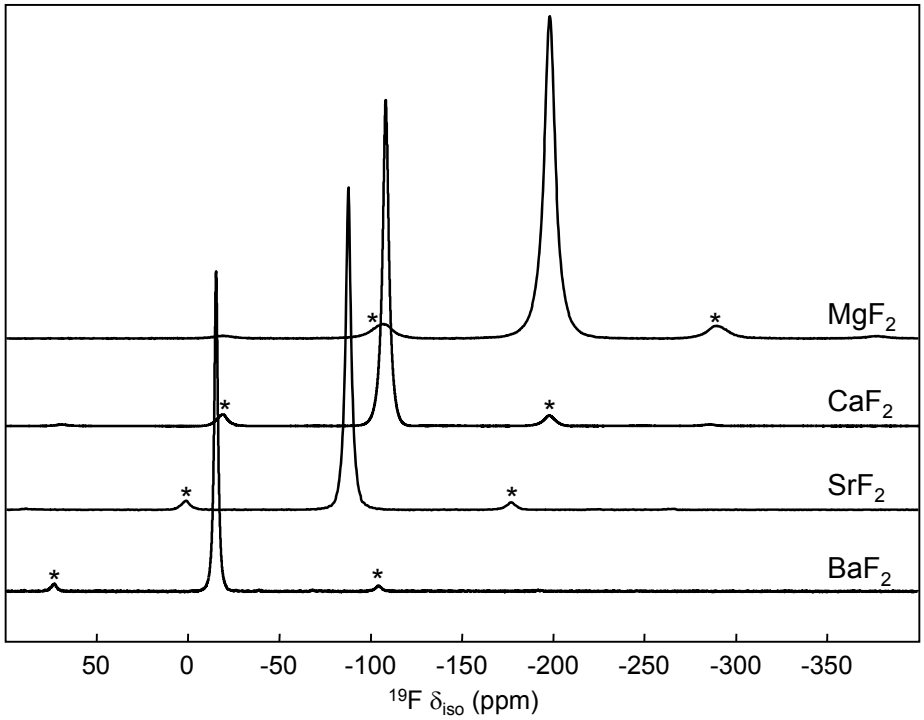

Figure S2. ^{19}F MAS NMR spectra of alkaline earth fluorides obtained at a magnetic field of 7.0 T using spinning frequencies of 25 kHz. The asterisks indicate spinning sidebands.

Solid state NMR and PXRD study of ScF_3

ScF_3 was recently studied by both ^{19}F and ^{45}Sc solid-state MAS NMR but the reported results[1] appear to us somewhat surprising and the results obtained in our study were also not straightforward to interpret.

Firstly, two different crystalline structures are reported for ScF_3 at ambient temperature and pressure: a cubic one[2,3] (ReO_3 type, space group: Pm-3m) and a rhombohedral one[4-6] (distorted ReO_3 type, space group: R32). Lo *et al.* report that their ScF_3 sample adopts a rhombohedral structure. However the small 2θ range of their powder X-ray diffraction (PXRD) pattern[1] does not allow confirming this assumption since both cubic and rhombohedral structures give very similar patterns, except for large 2θ values. The PXRD patterns recorded for our sample (Aldrich, 99.99%, lot number 04937HE) on the 2θ ranges 20-125°, 117.7-119.3°, 139.5-142.5° and 146.1-149.5° are shown in Figure 3. These diagrams do not evidence any rhombohedral splitting (Table 1) indicating that ScF_3 adopts a cubic structure at ambient temperature and pressure, in agreement with a recent study of the pronounced negative thermal expansion (NTE) of ScF_3.[7]

Both cubic and rhombohedral structures of ScF_3 contain a single Sc site and a single F site in the unit cell. Nevertheless, we were not able to reconstruct the ^{19}F MAS NMR spectrum with a single resonance (Figure 2). A satisfying reconstruction is obtained with three lines having close δ_{iso} values but significantly different chemical shift anisotropies (Table 2). Lo *et al.* report a δ_{iso} value equal to -35.9 ppm,[1] in good agreement with previously reported results,[8] and a CSA equal to ca. 305 ppm. This large value is in agreement with the observed intense spinning sidebands (the ^{19}F reconstructed spectrum is not presented).

Moreover, Lo *et al.*[1] estimated the ^{45}Sc quadrupolar coupling constant to 1.3(2) MHz and they claimed that "this small value is consistent with the high spherical symmetry around ^{45}Sc" whereas, as outlined by themselves, this nucleus has a moderately sized quadrupole moment ($Q = -0.22 \times 10^{-28}$ m^2).[9] We have also recorded a ^{45}Sc NMR spectrum of ScF_3 (Figure 3). Assuming a cubic structure, in which the Sc atom occupy the site with m-3m symmetry (1a Whyckoff position), a quadrupolar coupling constant equal to zero is expected. As Lo *et al.*[1], we observe a spinning sideband manifold, indicating quadrupolar frequency different from zero, and the shape of this spinning sideband manifolds likely

indicates some disorder in the structure. This spectrum is consequently difficult to reconstruct with a single set of parameters and the quadrupolar frequency can only be roughly estimated to 20 kHz (C_Q=280 kHz). Whereas the determined ^{45}Sc δ_{iso} value (-51.8 ppm) is very similar to the one determined by Lo et al. (-52 ppm), our quadrupolar coupling constant is significantly lower indicating less distorted Sc^{3+} sites.

At first glance, these results which can only be explained by the presence of some structural disorder in ScF_3 seem puzzling. Nevertheless, disorder was previously mentioned in ScF_3 to explain its marked NTE.[7] The assumed mechanism, *i. e.* rocking motion of essentially rigid ScF_6^{3-} octahedra, is supported by the large transverse component of the anisotropic displacement parameters (ADPs) for the fluoride anions.[7] ADPs may represent either atomic motion or static displacive disorder and static disorder was also invoked since it has been suggested for AlF_3 above its rhomboedral-to-cubic phase transition (the Al-F-Al links are locally bent in the cubic phase).[10,11] Both dynamic (depending on the motion frequency) and static disorders explain the non-zero quadrupolar frequency of ^{45}Sc (Figure 3) and the several lines used for the reconstruction of the ^{19}F NMR spectrum (Figure 2 and Table 2).

Local structural disorder in ScF_3 could also arise from incomplete fluorination leading to $ScF_{3-2x}O_x\square_x$ compounds and/or from occurrence of hydroxyl groups substituting fluoride ions into the network. Both these assumptions can be ruled out since the fluorinations of our sample, using either HF or F_2 at 600°C, do not lead to any changes on the NMR spectra.

Since several lines are used for the reconstruction of the ^{19}F NMR spectrum, ^{19}F δ_{iso} value for ScF_3 can only be roughly determined and the uncertainty is higher than for the others studied compounds. We choose the chemical shift value at the peak maximum, *i. e.* -36 ppm.

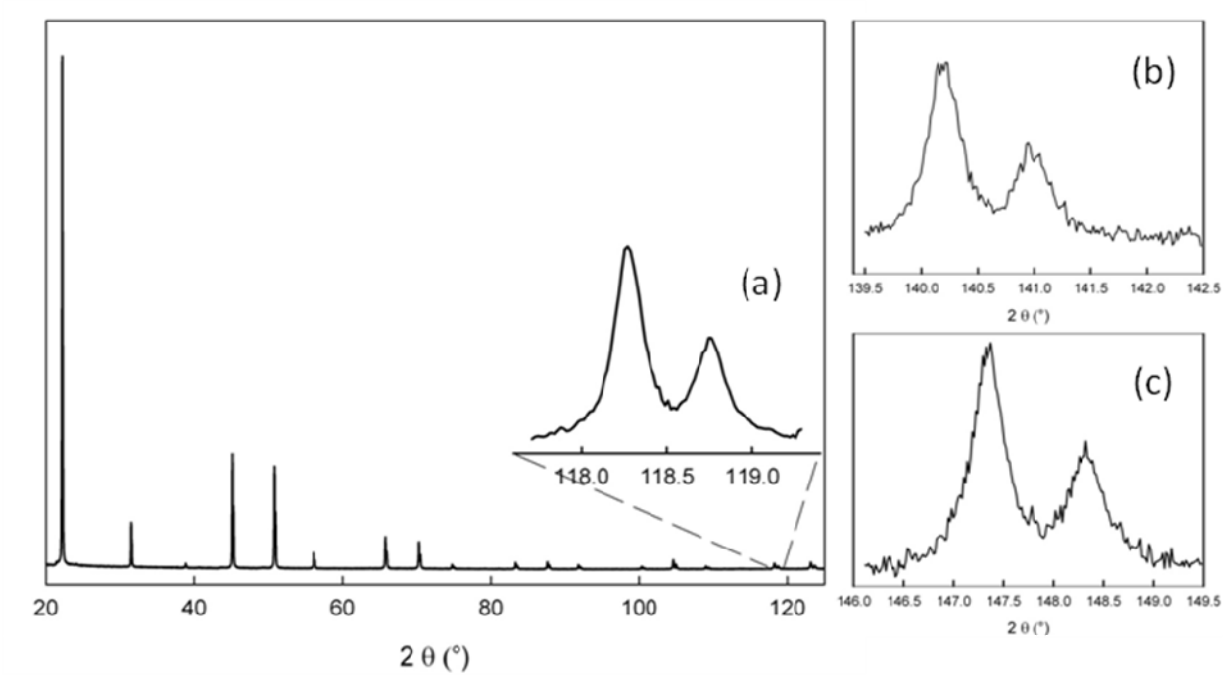

Figure S3. X-ray powder diffraction diagrams of ScF_3. In (a), (b) and (c) are shown the (4,2,0), (4,2,2) and (4,3,3) reflections, respectively. These diagrams were recorded under air, at room temperature with a PANalytical X'pert PRO diffractometer equipped with a X'Celerator detector using monochromated CuKα radiation (λ = 1.54056 Å). Measurements were done with an interpolated step of 0.017°, in the 2θ ranges 20-125°, (a) 117.7-119.3°, (b) 139.5-142.5° and (c) 146.1-149.5°, and total collecting times of 2 h 06 min, (a) 24 min, (b) 12 min and (c) 35 min.

Table S1. (h,k,l) reflections and corresponding 2θ values (°) of ScF_3 assuming Pm-3m[3] (ICSD[12] file number 36011) and R32[6] (ICSD[12] file number 77071) space groups (λ = 1.54056 Å).

Pm-3m				**R32**			
h	k	l	2θ	h	k	l	2θ
0	2	4	118.373	0	2	4	117.725
				-2	0	4	118.070
2	2	4	140.376	2	2	4	139.010
				-2	2	4	139.711
				-2	-2	4	139.948
0	3	4	147.565	0	3	4	146.189
0	0	5	147.565	0	0	5	146.602
				-3	0	4	147.019

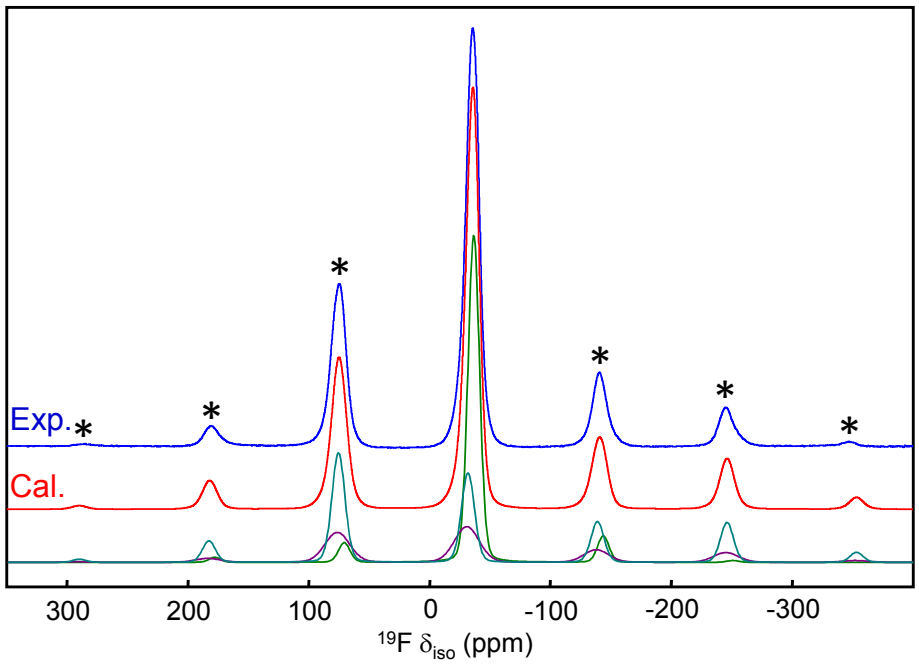

Figure S4. Experimental (exp.) and reconstructed (cal.) ^{19}F MAS NMR spectra of ScF_3 obtained at a magnetic field of 7.0 T using a spinning frequency of 30 kHz. The three individual contributions to the reconstructed spectrum are shown below. The asterisks indicate spinning sidebands.

Table S2. ^{19}F isotropic chemical shifts (δ_{iso}, ppm), chemical shift anisotropies (δ_{aniso}, ppm), asymmetry parameters (η), line widths and relative intensities (%) determined from the reconstruction of the ^{19}F NMR spectrum of ScF_3.

Line	δ_{iso} (±0.5)	δ_{aniso} (±10)	η (±0.05)	Width (±0.5)	Intensity (±0.5)
1	-36.5	107	0	11.2	40.7
2	-31.7	-279	0	12.7	38.0
3	-30.8	-322	0.2	24.1	21.3

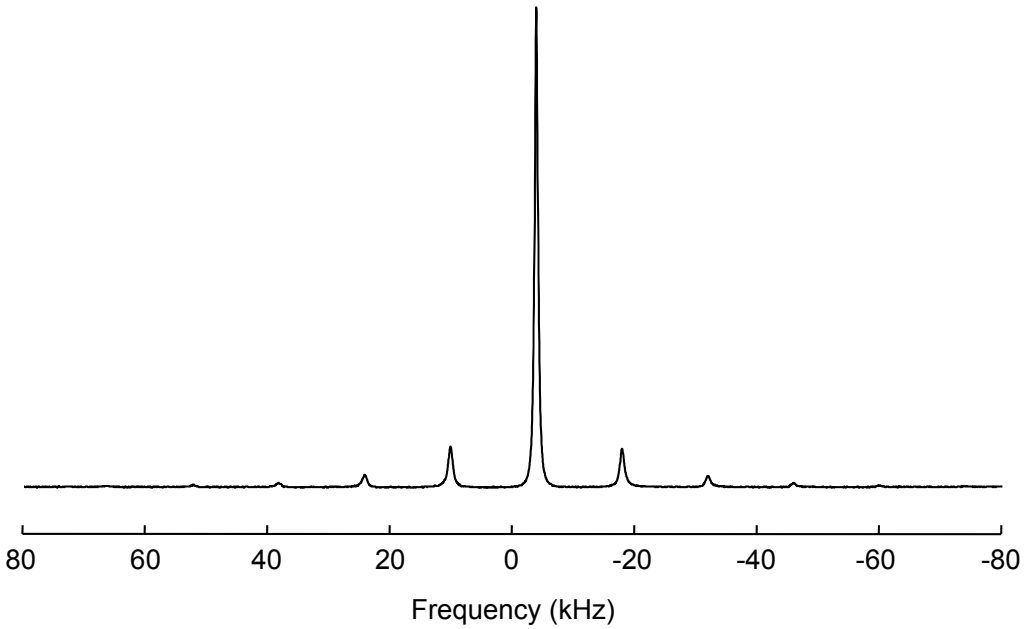

Figure S5. Experimental ^{45}Sc SATRAS (SAtellite TRAnsition Spectroscopy[13,14]) MAS NMR spectrum of ScF_3 recorded on a Bruker Avance 300 (7.0 T) spectrometer operating at a Larmor frequency of 72.906 MHz using a 2.5 mm probehead. The spinning frequency was 14 kHz. The quantitative excitation of all transitions[15] was ensured by using a short pulse duration (1 μs) with low-radio-frequency (RF) field strength (70 kHz). The recycle delay was set to 5 s. The ^{45}Sc chemical shift was referenced to a 1 M $Sc(NO_3)_3$ aqueous solution.

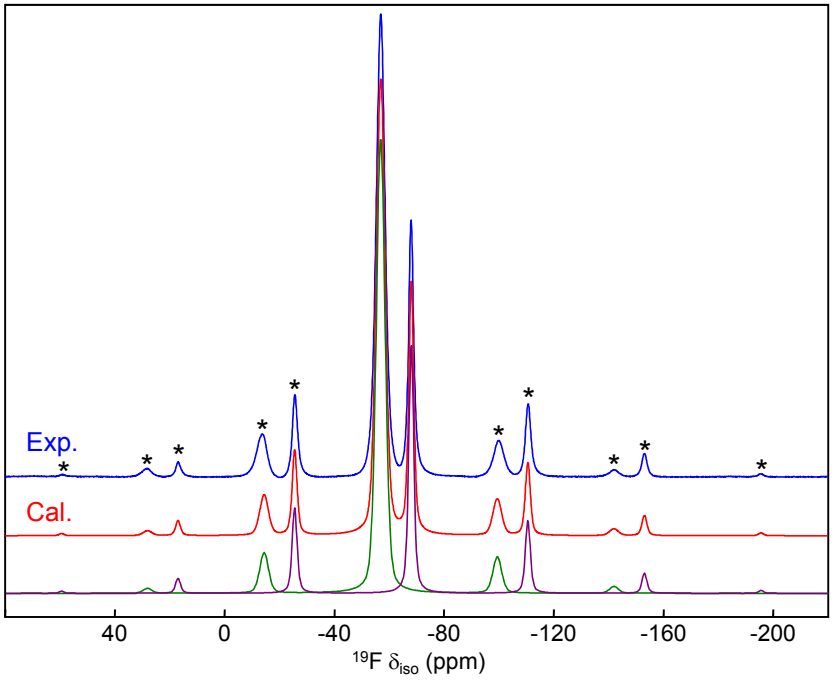

Figure S6. ^{19}F experimental (exp.) and reconstructed (cal.) ^{19}F MAS NMR spectra of YF_3 recorded at a magnetic field of 17.6 T using a spinning frequency of 30 kHz. The two individual contributions to the reconstructed spectrum are shown below. The asterisks indicate spinning sidebands.

Table S3. ^{19}F isotropic chemical shifts (δ_{iso}, ppm), chemical shift anisotropies (δ_{aniso}, ppm), asymmetry parameters (η), line widths (ppm), relative intensities (%) determined from the reconstruction of the ^{19}F NMR spectrum of YF_3 and line assignment.

Line	δ_{iso} (±0.2)	δ_{aniso} (±5)	η (±0.05)	Width (±0.1)	Intensity (±0.5)	Assignment
1	-56.9	-42.5	0.75	3.8	66.4	F2
2	-68.1	-76.5	0.80	2.1	33.6	F1

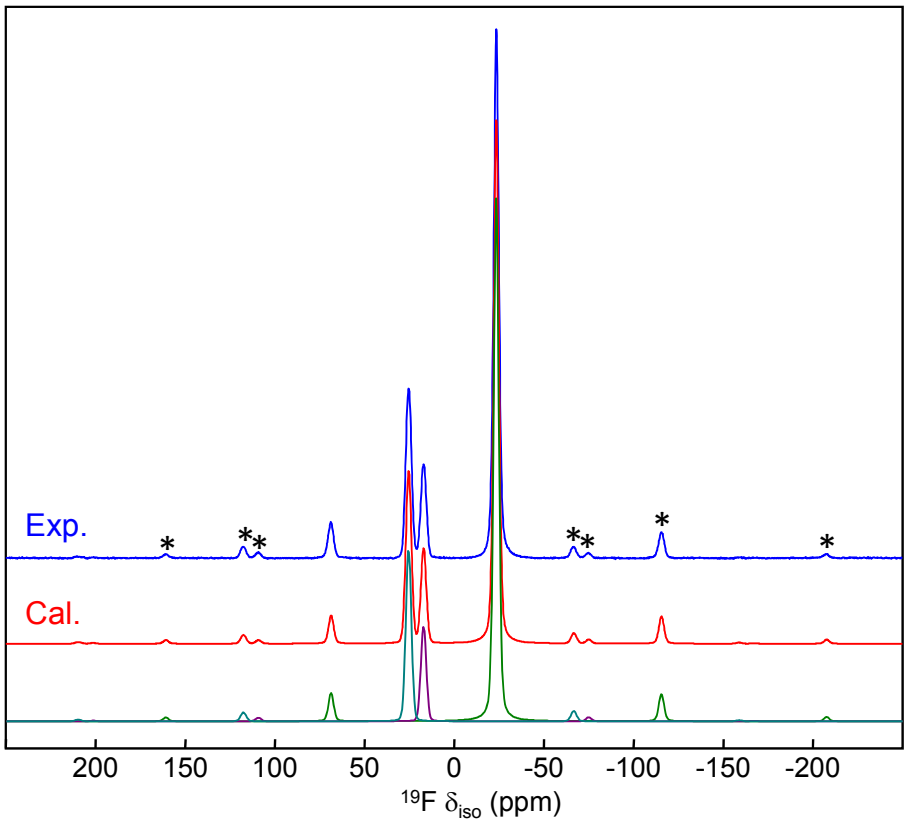

Figure S7. ^{19}F experimental (exp.) and reconstructed (cal.) MAS NMR spectra of LaF_3 recorded at a magnetic field of 17.6 T using a spinning frequency of 65 kHz. The three individual contributions to the reconstructed spectra are shown below. The asterisks indicate spinning sidebands.

Table S4. ^{19}F isotropic chemical shifts (δ_{iso}, ppm), chemical shift anisotropies (δ_{aniso}, ppm), asymmetry parameters (η), line widths (ppm), relative intensities (%) determined from the reconstruction of the ^{19}F NMR spectrum of LaF_3 and line assignment.

Line	δ_{iso} (±0.2)	δ_{aniso} (±5)	η (±0.05)	Width (±0.1)	Intensity (±0.5)	Assignment
1	-23.6	-71	0.9	3.3	66.7	F1
2	16.9	66	0.55	3.5	11.3	F3
3	25.3	78	0.55	3.6	22.0	F2

Table S5. Parameters used to generate the OTF USPP pseudopotentials. Details on the string can be found on the Castep website (http://www.castep.org/) in the documentation section.

Atom	**OTF USPP string**
F	2|1.4|16.537|18.375|20.212|20UU:21UU(qc=7.5)[]
Li	1|1.2|11|13.2|15|10U:20UU(qc=5.5)[]
Na	2|1.3|1.3|1.0|16|19|21|20UU:30UU:21U(qc=7)[]
K	2|1.8|1.8|1.6|11|14.7|16.7|30U:40UU:31UU(qc=5.5)[]
Rb	2|2.5|2.5|2.1|5.5|6.6|8.1|40U:50U+0U+0.125:41UU(qc=3.5)[]
Cs	2|2.7|2.7|1.6|4.4|5.9|7.4|50U:60U+0U+0.125:51UU(qc=3.5)[]
Mg	2|1.6|2|1.4|6|7|8|30NH:21U:31UU:32LGG(qc=4.5)[]
Ca	3|1.6|2|1.4|7.5|9.2|10.3|30U=-1.72:40U=-0.14: 31U=-1.03U=+0.25:32U=+0U=+1[]
Ca shift 1.81 eV	3|1.6|2|1.4|7.5|9.2|10.3|30U=-1.72:40U=-0.14: 31U=-1.03U=+0.25:32U=+0@+0.0665U=+1@+0.0665[]
Sr	3|2|2|1.2|7.4|9.2|11|40U:50U:41UU:42UU[]
Ba	2|3|2.9|2.2|6.4|8.1|9|50U:60UU:51U2.5U2.5(qc=3.5)[]
Sc	3|1.8|1.8|1.6|9.6|10.8|11.7|30U=-2.01:40U=-0.16: 31U=-1.235U=+0.25:32U=-0.125U=+0.25[]
Sc shift 1.96 eV	3|1.8|1.8|1.6|9.6|10.8|11.7|30U=-2.01:40U=-0.16: 31U=-1.235U=+0.25: 32U=-0.125@0.0720U=+0.25@0.0720[]
La	2|2|2|1.4|8|12|13|50N:60NH:51UU:52LGG: 43U1.6+0U1.6+0.1{5d0.9,4f0.1}(qc=6)[]
La shift 4.55 eV	2|2|2|1.4|8|12|13|50N:60NH:51UU:52LGG: 43U1.6+0@0.1672U1.6+0.1@0.1672{5d0.9,4f0.1}(qc=6)[]
Y	3|2|2|2|8.5|10|11.1|40U:50U:41UU:42UU[]

Table S6. Fractional atomic coordinates from the initial (IS)[16] and and PBE-DFT geometry-optimized (APO) structures for MgF_2.

Atom	Site		*x*	*y*	*z*
Mg	2a		0	0	0
F	4f	*IS*	*0.3028*	*0.3028*	*0*
		APO	0.3022	0.3022	0

Table S7. Mg-F bond lengths and F-Mg-F bond angles deduced from the initial[16] (IS) and PBE-DFT geometry-optimized (APO) structures for MgF_2.

Bond lengths/Å		Bond angles/°	
IS	APO	IS	APO
1.979	1.975	81.04	81.22
1.984	1.986	98.96	98.78

Table S8. Eigenvectors of the calculated ^{25}Mg EFG tensor, after optimization, expressed in Cartesian coordinates for MgF_2 at the (0,0,0) position. The definition of the Cartesian axis with respect to the lattice parameters is given below.

Axis	V_{xx}	V_{yy}	V_{zz}
i	0.7071	0	-0.7071
j	0.7071	0	0.7071
k	0	1	0

With $\begin{pmatrix} a \\ b \\ c \end{pmatrix} = \begin{pmatrix} 4.6213 & 0.0000 & 0.0000 \\ 0.0000 & 4.6213 & 0.0000 \\ 0.0000 & 0.0000 & 3.0159 \end{pmatrix} \times \begin{pmatrix} i \\ j \\ k \end{pmatrix}$

and $a = b = 4.6213$ Å, $c = 3.0159$ Å ; $\alpha = \beta = \gamma = 90°$

Table S9. Fractional atomic coordinates from the initial (IS)[17] and PBE-DFT geometry-optimized (APO) structures for YF_3.

Atom	Site		*x*	*y*	*z*
Y	4c	*IS*	*0.3673*	*1/4*	*0.0591*
		APO	0.3687	1/4	0.0604
F1	4c	*IS*	*0.5227*	*1/4*	*0.5910*
		APO	0.5231	1/4	0.5906
F2	8d	*IS*	*0.1652*	*0.0643*	*0.3755*
		APO	0.1655	0.0629	0.3775

Table S10. Y-F bond lengths deduced from the initial[17] (IS) and PBE-DFT geometry-optimized (APO) structures for YF_3.

Bond lengths/Å	IS	APO
Y-F1	2.282	2.285
	2.287	2.294
	2.538	2.528
Y-F2	2.281 (x2)	2.291 (x2)
	2.299 (x2)	2.296 (x2)
	2.310 (x2)	2.299 (x2)

Table S11. Fractional atomic coordinates from the initial (IS)[18] and PBE-DFT geometry-optimized (APO) structures for LaF_3.

Atom	Site		x	y	z
La	6f	*IS*	*0.6598*	*0*	*1/4*
		APO	0.6578	0	1/4
F1	12g	*IS*	*0.3659*	*0.0536*	*0.0813*
		APO	0.3688	0.0584	0.0805
F2	4d	*IS*	*1/3*	*2/3*	*0.1830*
		APO	1/3	2/3	0.1825
F3	2a		0	0	1/4

Table S12. La-F bond lengths deduced from the initial[18] (IS) and PBE-DFT geometry-optimized (APO) structures for LaF_3.

Bond lengths/Å	IS	APO
La-F1	2.458 (x2)	2.457 (x2)
	2.489 (x2)	2.477 (x2)
	2.638 (x2)	2.629 (x2)
	3.003 (x2)	3.038 (x2)
La-F2	2.417 (x2)	2.415 (x2)
La-F3	2.444	2.458

Table S13. Eigenvectors of the calculated ^{139}La EFG tensor in LaF_3 for IS, expressed in a Cartesian coordinate system (*i, j, k*) and along the crystallographic axis (*a, b, c*) for the La position at (0.6578, 0, 1/4). The definition of the Cartesian axis with respect to the lattice parameters is given below.

Axis	V_{xx}	V_{yy}	V_{zz}
i	0.2880	-0.8660	-0.4087
j	0.4989	0.5	-0.7079
k	0.8174	0	0.5761
a	0.0466	-0.1391	-0.0654
b	0.0933	0.0000	-0.1308
c	0.1106	0.0000	0.0789

With $\begin{pmatrix} a \\ b \\ c \end{pmatrix} = \begin{pmatrix} 6.2224 & -3.5925 & 0 \\ 0 & 7.1850 & 0 \\ 0 & 0 & 7.3510 \end{pmatrix} \times \begin{pmatrix} i \\ j \\ k \end{pmatrix}$

and $a = b = 7.1850$ Å, $c = 7.3510$ Å ; $\alpha = \beta = 90°$, $\gamma = 120°$

Table S14. Experimental ^{19}F isotropic chemical shifts relative to $CFCl_3$ and calculated ^{19}F isotropic shieldings for the eleven compounds additionally considered in Figure 5. The "calculated" ^{19}F isotropic chemical shifts according to $\delta_{iso}/CFCl_3 = -0.80(3)\ \sigma_{iso} + 89(9)$ are also reported.

Compounds	Site	$\sigma_{iso}^{calc.}$ (ppm)	$\delta_{iso}^{calc.}$ (ppm)	$\delta_{iso}^{exp.}$ (ppm)
CdF_2	F1	350.9[a]	-192	-190.7[c]
HgF_2	F1	356.4[a]	-196	-197.6[d]
α-PbF_2	F1	140.8[a]	-24	-20.5[e]
	F2	176.6[a]	-52	-57.7[e]
α-AlF_3	F1	336.2[a]	-180	-172.0[f]
$Na_5Al_3F_{14}$	F1	358.9[a]	-198	-191.4[g]
	F2	326.1[a]	-172	-165.0[g]
	F3	356.9[a]	-197	-189.5[g]
ZnF_2	F1	363.0[b]	-201	-200.7[c]
GaF_3	F1	314.0[b]	-162	-167.2[c]
InF_3	F1	364.1[b]	-202	-206.2[c]
$BaLiF_3$	F1	238.8[b]	-102	-98.2[c]
β-$BaAlF_5$	F1	307.4[b]	-157	-154.6[h]
	F2	287.9[b]	-141	-138.9[h]
	F3	268.5[b]	-126	-121.3[h]
	F4	254.9[b]	-115	-109.2[h]
	F5	302.4[b]	-153	-148.8[h]
	F6	277.5[b]	-133	-127.5[h]
	F7	293.3[b]	-146	-140.8[h]
	F8	245.4[b]	-107	-99.0[h]
	F9	271.7[b]	-128	-124.5[h]
	F10	297.0[b]	-149	-144.6[h]
$Ba_3Al_2F_{12}$	F1	310.9[b]	-160	-153.3[h]
	F2	308.2[b]	-158	-151.6[h]
	F3	165.1[b]	-43	-30.5[h]
	F4	186.6[b]	-60	-50.8[h]
	F5	267.6[b]	-125	-115.7[h]
	F6	265.4[b]	-123	-113.0[h]
	F7	279.8[b]	-135	-127.9[h]
	F8	302.3[b]	-153	-146.4[h]

[a] Calculated values from reference [19].
[b] Calculated values from reference [20].
[c] Experimental values from reference [21].
[d] Experimental values from reference [22].
[e] Experimental values from reference [23].
[f] Experimental values from reference [24].
[g] Experimental values from reference [25].
[h] Experimental values from reference [26].

References

[1] A. Y. H. Lo, V. Sudarsan, S. Sivakumar, F. van Veggel, R. W. Schurko, *J. Am. Chem. Soc.* 2007, **129**, 4687.
[2] K. H. Jack, *Acta Cryst.* 1957, **10**, 780.
[3] P. P. Fedorov, V. Trncova, G. I. Kocherba, B. P. Sobolev, *Kristallografiya* 1995, **40**, 716 ; *Crystallogr. Rep.* 1995, **40**, 663.
[4] W. Nowacki, *Z. Kristallogr. Kristallgeom. Kristallphys. Kristallchem.* 1939, **101**, 273.
[5] E. G. Ippolitov, A. G. Maklachkov, *Inorg. Mater. (Engl. Transl.)* 1970, **6**, 1251.
[6] R. Loesch, C. Hebecker, Z. *Z.* Ranft, *Anorg. Allg. Chem.* 1982, **491**, 199.
[7] B. K. Greve, K. L. Martin, P. L. Lee, P. J. Chupas, K. W. Chapman, A. P. Wilkinson, *J. Am. Chem. Soc.* 2010, **132**, 15496.
[8] L. M. Avkhutskii, Y. V. Gagarinskii, S. A. Polishchuk, S. P. Gabuda, *Spectrosc. Lett.* 1969, **2**, 75.
[9] P. Pyykko, *Mol. Phys.* 2001, **99**, 1617.
[10] S. Chaudhuri, P. J. Chupas, M. Wilson, P. Madden, C. P. Grey, *J. Phys. Chem. B* 2004, **108**, 3437.
[11] P. J. Chupas, S. Chaudhuri, J. C. Hanson, X. Qiu, P. L. Lee, S. D. Shastri, S. J. L. Billinge, C. P. Grey, *J. Am. Chem. Soc.* 2004, **126**, 4756.
[12] Inorganic Crystal Structure Database (ICSD), version 1.7.1, 2010.
[13] J. Skibsted, N. C. Nielsen, H. Bildsoe, H. J. Jakobsen, *J. Magn. Reson.*, 1991, **95**, 88.
[14] B. B. C. Jäger, in *Solid State NMR II*, (Ed.: B. Blümich), Springer-Verlag: Berlin, 1994, 163.
[15] A. Samoson, E. Lippmaa, *Phys. Rev. B*, 1983, **28**, 6567.
[16] W. H. Baur, A. A. Khan, *Acta Crystallogr.* 1971, **B27**, 2133.
[17] A. K. Cheetham, N. Norman, *Acta Chem. Scand. Ser. A* 1974, **28**, 55.
[18] A. Zalkin, D. H. Templeton, *Acta Crystallogr.* 1985, **B41**, 91.
[19] J. M. Griffin, J. R. Yates, A. J. Berry, S. Wimperis, S. E. Ashbrook, *J. Am. Chem. Soc.* 2010, **132**, 15651.
[20] A. Zheng, S.-B. Liu, and F. Deng, *J. Phys. Chem. C* 2009, **113**, 15018.
[21] B. Bureau, G. Silly, J.-Y. Buzaré, J. Emery, *Chem. Phys*. 1999, **249**, 89.
[22] A. T. Kreinbrink, C. D. Sazavsky, J. W. Pyrz, D. G. A. Nelson, S. R. Honkonen, *J. Magn. Reson.* 1990, **88**, 267.
[23] F. Wang, C. P. Grey, *J. Am. Chem. Soc.* 1998, **120**, 970.
[24] P. J. Chupas, M. F. Ciraolo, J. C. Hanson, C. P. Grey, *J. Am. Chem. Soc.* 2001, **123**, 1694.
[25] L.-S. Du, A. Samoson, T. Tuherm, C. P. Grey, *Chem. Mater.* 2000, **12**, 3611.
[26] C. Martineau, C. Legein, J.-Y. Buzaré, F. Fayon, *Phys. Chem. Chem. Phys.* 2009, **11**, 950.